Sustainable Materials and Technologies 45 (2025) e01619

Contents lists available at ScienceDirect

Sustainable Materials and Technologies

journal homepage: www.elsevier.com/locate/susmat

Silica-supported ionic liquids as efficient materials to separate cobalt and nickel from lithium in aqueous solutions☆

Joana C. Almeida [a,b], Celso E.D. Cardoso [a,b], Rosa Freitas [c], Tito Trindade [a], Mara G. Freire [a], Eduarda Pereira [b,*]

[a] Chemistry Department and CICECO-Aveiro Institute of Materials, University of Aveiro, Campus de Santiago, 3810-193 Aveiro, Portugal
[b] Chemistry Department and LAQV-REQUIMTE, University of Aveiro, Campus de Santiago, 3810-193 Aveiro, Portugal
[c] Biology Department and CESAM, University of Aveiro, Campus de Santiago, 3810-193 Aveiro, Portugal

ARTICLE INFO

Keywords:
Metal ions
Box-Behnken design
Process optimization
Sorption
Supported ionic liquids

ABSTRACT

Lithium (Li^{+}), cobalt (Co^{2+}), and nickel (Ni^{2+}) are critical elements used in various types of lithium-ion batteries, including those in electric vehicles and other industrial applications. Given the increasing demand for these materials and their risk of scarcity, it is important to develop technologies that can efficiently extract these metals from secondary sources, such as industrial effluents, rather than focusing solely on spent batteries. This study addresses the preparation and evaluation of an imidazolium-based supported ionic liquid (SIL) for the selective removal of citrate-coordinated Co^{2+} and Ni^{2+} from aqueous solutions, obtaining a solution predominantly containing Li^{+}. Optimal sorption conditions were identified using Response Surface Methodology (RSM), with pH 7.8, 1.5 g/L SIL, and 0.4 mg/L metals yielding removal efficiencies of 95 % of Co^{2+} and Ni^{2+} in just 2 h. The SIL showed high performance in ultra-pure and bottled waters, but efficiency declined in saline matrices due to the competition with other ions. Ecotoxicity tests using the bioindicator species *Mytilus galloprovincialis* revealed no adverse effects at concentrations up to 1 g/L. These results demonstrate the SIL's potential for sustainable and selective recovery of critical metals from low-salinity industrial effluents and other secondary aqueous sources.

1. Introduction

The growing demand for lithium-ion batteries (LIBs) has been driven by various industries, including automotive and electronics. These batteries typically contain metals such as lithium (Li^{+}), cobalt (Co^{2+}), and nickel (Ni^{2+}), which are essential for their performance. Although the automotive industry has contributed significantly to the rise in LIB production [1], these metals are also widely used in batteries for other applications, such as consumer electronics and industrial machinery. The increasing demand for these critical materials raises concerns about their long-term availability. Extracting these metals is not only expensive but also energy-intensive, with detrimental environmental impacts [2,3]. As a result, there is a pressing need for research into alternative resources, such as industrial effluents, to further mitigate these issues and promote sustainability [2,4]. Hydrometallurgical processes, commonly used to recover metals from spent LIBs [5], also offer a promising approach for extracting metals from other secondary sources, such as industrial effluents. However, these processes often involve volatile organic compounds and hazardous chemicals, leading to environmental problems [5,6].

Numerous strategies have been explored for the removal of metal ions from aqueous solutions, with sorption emerging as one of the most effective and widely applied techniques due to its operational simplicity, low cost, and high efficiency [7]. Various sorbent materials have shown strong potential for removing critical metals such as Li^{+}, Co^{2+}, and Ni^{2+}, including natural biosorbents like algae and soybean biomass [8,9], inorganic oxides such as hydrous zirconium oxide [10], silica-based materials [11], activated carbons [12], and functionalized polymers or ion-exchange resins [13]. Marine algae biomass, for example, can sorb metal ions like Co^{2+} from aqueous solutions and allow their efficient recovery through desorption; however, biosorption capacity decreases significantly after the first reuse [9]. Hydrous zirconium oxide hybrid materials have demonstrated high affinity for Ni^{2+}, but their performance is limited to a narrow pH range of 6.0–7.5, with reduced sorption

☆ This article is part of a Special issue entitled: 'Responsible Li Production' published in Sustainable Materials and Technologies.

* Corresponding author.
E-mail address: eduper@ua.pt (E. Pereira).

https://doi.org/10.1016/j.susmat.2025.e01619
Received 10 January 2025; Received in revised form 9 July 2025; Accepted 21 August 2025
Available online 22 August 2025

at more acidic or basic conditions [10]. Similarly, mesoporous silica has shown promising results for Co^{2+} removal, achieving up to 89 % efficiency under optimal conditions; however, it requires long contact times (up to 8 h) to reach effective sorption levels [11]. Despite their high affinities for metal ions, these materials often face challenges such as limited reusability after desorption, sensitivity to narrow pH ranges, and slow sorption kinetics requiring extended contact times. Recently, ionic liquids (ILs) and supported ionic liquids (SILs) have gained attention due to their high sorption selectivity, fast kinetics and tunable properties [14,15].

The use of SILs in removal and recovery processes is considered an eco-friendly alternative to hydrometallurgical processes [16,17]. Compared to conventional solvents, ILs and SILs offer higher extraction and sorption performances with lower environmental impact [17]. ILs also exhibit high chemical and thermal stability compared to organic solvents, and possess low vapor pressure which leads to a lower risk of environmental contamination [17,18]. Furthermore, their performance can be improved through the combination of different anions and cations, obtaining ILs with customizable chemical and physical properties [18]. Nevertheless, the application of ILs in liquid-liquid extraction may present some limitations, namely low diffusion coefficients, high viscosity of some ILs, and difficulties in solvent recycling and product purification [19]. Immobilizing of ILs onto solid supports, like silica-gel, allows not only to overcome these limitations, but also to reduce the ILs cost since there is a reduction of the amount of the required IL compared to conventional liquid−liquid separation [19]. Moreover, silica-gel is an environmentally friendly and low cost material. Thus, the unique properties of ILs, when combined with the benefits of solid supports, have generated significant interest in using SILs as alternative materials for metals extraction. These features make SILs promising candidates for application in industrial effluent treatment and secondary resource recovery systems. Their potential for selective separation of critical metals under mild conditions supports the development of more sustainable and scalable metal recovery processes.

Despite the demonstrated efficiency of ionic liquids in extracting Li^{+}, Co^{2+}, and Ni^{2+} from chloride solutions [20], to the best of our knowledge, only two studies have used SILs as sorbents for the removal of cobalt [21,22], and none have focused on lithium or nickel. Moreover, the information about their environmental impact and potential ecotoxicity is scarce [23,24]. When used in removal processes, ILs and SILs can reach aquatic systems and, therefore, it is important to evaluate their toxicity. Several studies have addressed the toxicological evaluation of ILs to aquatic organisms [24–26]. These studies indicate that their toxicity is mainly associated with the cation alkyl chain length, which also determines the lipophilicity of the compound. Compared to the cation's toxic effects, the influence of the anion is almost negligible [24]. Bivalves have been widely used for biomonitoring of environmental pollution and ecotoxicological assessment because of their abundance, wide spatial distribution, and ecological and economic relevance [27]. Accordingly, the mussel species *Mytilus galloprovincialis* was selected for this study to evaluate the toxic effects caused by the SIL used.

Statistical tools, like Design of Experiments (DoE) and Response Surface Methodology (RSM), have been explored here to optimize the sorption processes [28–30]. Firstly, the effects of selected experimental variables on the sorption process studied by DoE allows to understand which of them significantly affect the response variable and, thus, which are most important to consider in subsequent studies [28]. RSM is subsequently used on the experimental data obtained from the DoE to develop a statistical model that explains the relationship between the variables and the response. One of the most used methods to perform DoE is the Box-Behnken design. This approach requires a reduced number of experiments, making the procedure more efficient, and provides high precision in determining optimal conditions. However, at extreme points and outside the experimental region, the prediction quality decreases, and the behavior of the response may not be accurately captured [30–32].

Hence, the main aims of this study were: (i) to prepare and characterize (chemically and morphologically) a SIL with an imidazolium cation and chloride as counter-ion; ii) to investigate the impact of various experimental factors (solution medium, time, citrate concentration, initial metals concentration, dose of sorbent and pH) on the removal of Li^{+}, Co^{2+} and Ni^{2+} species from waters by applying the Box-Behnken design; (iii) to develop a model that describes the removal process under the tested conditions and to identify the optimal parameters for the extraction of the target metals; (iv) to assess the performance of the SIL on more complex matrices; and (v) to assess the ecotoxicological safety of the SIL by evaluating its effects on the model species *M. galloprovincialis*.

2. Experimental section

2.1. Materials

Chemicals were supplied by commercial sources and used without further purification: (3-chloropropyl)trimethoxysilane (>98 %, Acros Organics), cobalt (Co^{2+} in 2–5 % HNO_3, 1000 mg/L, VWR Chemicals), cobalt sulphate heptahydrate ($CoSO_4.7H_2O$, 99 %, Carlo Erba), cobalt chloride hexahydrate ($CoCl_2{\cdot}6H_2O$, 98 %, Panreac), ethanol (C_2H_5OH, 99.9 %, Carlo Erba), hydrochloric acid (37 %, Sigma Aldrich), lithium chloride (LiCl, >99 %, Sigma Aldrich), methanol (HPLC grade, Fisher Scientific), nickel chloride hexahydrate ($NiCl_2{\cdot}6H_2O$, >97 %, Riedel-de Haën), nitric acid (HNO_3, puriss. p.a., 65 %, Merck), *N*-methylimidazole (99 %, Acros Organics), potassium hydroxide (KOH, >98 %, Pronolab), potassium nitrate (KNO_3, >99 %, Merck), silica-gel particles (90 Å, 0.2–0.5 mm, Fluka), sodium hydroxide (NaOH, >98 %, Pronolab), trisodium citrate dihydrate ($C_6H_5Na_3O_7{\cdot}2H_2O$, >99 %, Panreac), and toluene (99.8 %, Fisher Scientific). The water used in the sorption experiments was double distilled, passed across a reverse osmosis system and further treated with a Milli-Q plus 185 water purification equipment. The synthetic seawater solutions (with salinity 15 and 30) were prepared by diluting the required amount of the artificial salt tropic Marin® SEA SALT in distilled water, obtained from Tropic Marine Center.

2.2. Synthesis of the imidazolium-based SIL ([Si][C_3C_1Im]Cl)

The synthesis procedure of [Si][C_3C_1Im]Cl used in the present study, adapted from Qiu et al. [33], is described in Bernardo et al. [15] and provided in the Supporting Information.

2.3. Characterization techniques

The physical and chemical characterization of the prepared SIL was conducted using a variety of techniques. Solid State ^{13}C Nuclear Magnetic Resonance (NMR) spectra were acquired at 9.7 T on a Bruker Avance III – 400 MHz spectrometer on a 4 mm BL cross-polarization magic angle spinning (CPMAS) VTN probe at 100.6 MHz, at room temperature, using the following parameters: recycle delay, 5 s; contact time, 3.5 ms; $\nu_R = 12$ kHz. SPINAL-64 decoupling was used during data acquisition. Fourier Transform Infrared (FT-IR) spectra (in the range 4000–350 cm^{-1}) were recorded using a Bruker Tensor 27 spectrophotometer, equipped with an Attenuated Total Reflectance (ATR) accessory, after 256 scans with resolution of 4 cm^{-1}. Elemental analysis for carbon, hydrogen, nitrogen and sulfur contents (in weight percentage) was performed with a Truspec Micro CHNS 630–200-200 elemental analyser. Analysis parameters were the following: sample amount about 2 mg; combustion furnace temperature of 1075 °C; afterburner temperature of 850 °C. Infrared absorption was used to determine the amount of carbon and hydrogen, while the amount of nitrogen was determined by thermal conductivity. The specific surface area (S_{BET}) of silica and SILs was determined using an automated surface area analyser

(Quantachrome Autosorb IQ2) by means of nitrogen adsorption-desorption. Prior to the measurements, the samples were degassed overnight at 100 °C. *zeta* potential measurements of the colloidal samples were performed using a Zetasizer Nano ZS (Malvern Instruments). The pH of the colloid varied between 2 and 10, either using NaOH or HNO_3 aqueous solutions. The temperature was kept at 25 °C, and three replicate measurements of the zeta potential were performed for each sample.

2.4. Sorption experiments

Sorption experiments were designed to assess the ability of the prepared SIL to sorb Li^+, Co^{2+} and Ni^{2+} ions from aqueous solutions under varying physicochemical conditions. All assays were carried out in 1000 mL Schott flasks with agitation at 250 rpm and room temperature on a mechanical shaker, and for a contact time of 2 h unless stated otherwise. Control solutions, consisting of ultra-pure water containing only the chemical elements (without the sorbent), were run in parallel with each assay to assess possible experimental losses of Li^+, Co^{2+}, and Ni^{2+} due to precipitation, sorption on the vessel walls, or contamination. The amount of Li^+, Co^{2+} and Ni^{2+} was quantified by Inductively Coupled Plasma-Optical Emission Spectrometry (ICP-OES), as described in the Supporting Information.

Influence of anionic media and sorption time was first investigated using synthetic single-element cobalt solutions prepared in three different media: chloride (from $CoCl_2·6H_2O$), sulphate (from $CoSO_4·7H_2O$), and nitrate (from a commercial Co^{2+} standard solution in HNO_3). Each 1000 mL solution was adjusted to contain 1 mg/L of Co^{2+}, and trisodium citrate was added to a final concentration of 0.001 mol/L to promote metal complexation. The initial pH was set to 6.0 using dilute NaOH or HNO_3 solutions. Then, 500 mg of SIL was added to each flask (0.5 g/L final concentration), and samples were collected at selected time intervals up to 24 h to evaluate kinetic behavior. After sorption, the SIL particles were separated via centrifugation at 5000 rpm for 4 min. Supernatants were acidified to pH < 2 with 65 % HNO_3 and stored at 4 °C until analysis.

Effect of citrate concentration was investigated in a multi-element solution (Li^+, Co^{2+} and Ni^{2+} at 1 mg/L each) prepared in ultra-pure water using LiCl, $CoCl_2·6H_2O$ and $NiCl_2·6H_2O$. Four different trisodium citrate concentrations were tested: 0, 0.001, 0.01, and 0.1 mol/L. Each solution (1000 mL) was adjusted to pH 6.0, and 500 mg of SIL was added. After 2 h of contact time under the same agitation and temperature conditions, samples were centrifuged, acidified, and preserved for analysis as above.

Optimization of sorption parameters was performed using a Box-Behnken experimental design considering three factors: solution pH (4, 6, 8), SIL dose (0.5, 1.0, 1.5 g/L), and initial metal concentration (0.4, 1.2, 2.0 mg/L for each Li^+, Co^{2+} and Ni^{2+}), as detailed in Table 1. The concentration range (0.4–2.0 mg/L) was selected to reflect typical scenarios encountered in final polishing stages of industrial effluent treatment, where metal concentrations are already low but still exceed regulatory thresholds. For example, municipal wastewater in Thessaloniki (Greece) contained 0.7 mg/L of Ni^{2+} [34]. Also, a recent study reported Ni^{2+} concentrations up to 0.86 mg/L in textile industry effluents and Co^{2+} concentrations between 1.12 and 3.17 mg/L in chemical and tannery industry discharges [35]. At these levels, traditional treatment methods become less effective, and advanced materials like SILs offer a selective and efficient alternative. Citrate anions were introduced to all aqueous solutions (0.0004, 0.0012 and 0.002 mol/L), according to the metal solution concentrations. Each 1000 mL solution was adjusted to the desired pH using 2 % (*v*/v) HNO_3 or NaOH solutions (1 and 10 mol/L). Sorbent was added, and the mixture was stirred for 2 h before separation, acidification, and preservation for ICP-OES analysis. Table S1 (in the Supporting Information) displays the experiments generated by Box-Behnken design. The central point was performed 3 times to improve the precision of the model.

Matrix complexity was evaluated by repeating optimal conditions (identified by Response Surface Methodology) in three types of water: ultra-pure water, commercial bottled mineral water, and synthetic seawater at salinities of 15 and 30 (prepared using Tropic Marin® salts).

Table 1
Experimental conditions for the three factors studied and the three-level conditions.

Variable	Level		
	-1	0	1
pH	4	6	8
Dose of sorbent (g/L)	0.5	1.0	1.5
Concentration of Li^+, Co^{2+} and Ni^{2+} (mg/L)	0.4	1.2	2.0

2.5. Exposure assay of the SIL to mussels

Mussels of similar size (length: 63.6 ± 3.3 mm; width: 36.5 ± 2.4 mm) were collected, acclimated to the laboratory conditions, and acutely exposed for seven days to control (CTL, seawater without SIL, salinity 30) and SIL presence (25, 50, 100, 250, 500 and 1000 mg/L of SIL) at room temperature. Three replicates, each consisting of 3 L aquaria and containing five mussels, were used for each treatment. The concentrations of SIL selected for this study were in the same range as those used in the sorption experiments. At the end of the experimental period, the mussels were individually frozen using liquid nitrogen and stored at −80 °C until they could be manually homogenized. The entire soft tissue of each mussel was homogenized using a mortar and pestle under liquid nitrogen to assess the overall health of the specimens. Each mussel was then divided into three 0.5 g fresh weight (FW) aliquots for biomarker analysis, with the remaining tissue being stored. The biochemical endpoints assessed were: 1) metabolic capacity measured by electron transport system (ETS) activity; 2) energy reserves assessed by the total protein (PROT) content; 2) antioxidant defenses measured by superoxide dismutase (SOD) activity; and 3) cellular damage determined by lipid peroxidation (LPO) levels.

Each biochemical assay was conducted according to the methodology described by Andrade et al. [36]. The extraction procedure is described in the Supporting Information.

3. Results and discussion

3.1. Characterization of imidazolium-based SIL

The successful synthesis of the imidazolium-based SIL was confirmed using solid-state ^{13}C NMR spectroscopy, as shown in Fig. 1. The ^{13}C NMR spectrum of the [Si][C_3]Cl intermediate shows three peaks at 10, 26 and 47 ppm, which correspond to the three carbon atoms of the propyl alkyl chain. In the ^{13}C NMR spectrum of [Si][C_3C_1Im]Cl, peaks are observed for the carbons in the imidazolium ring at 123–124 and 137 ppm, the methyl chain carbon at 37 ppm, and the carbons in the propyl chain at 9, 24 and 52 ppm. The ^{13}C NMR spectrum of the SIL produced by reacting chloropropyl silica with *N*-methylimidazole cation is in agreement with previous works [14,15].

The functionalization of [Si][C_3C_1Im]Cl was further confirmed through the FTIR spectra acquired for activated silica, [Si][C_3]Cl and [Si][C_3C_1Im]Cl (Fig. S1 in the Supporting Information). In the FTIR spectrum of [Si][C_3C_1Im]Cl, a weak band at 1574 cm^{-1} is observed, which is associated with the vibration of the imidazole ring [15].

Table 2 provides the elemental analysis results for several samples. Carbon and hydrogen detected in the intermediate material, i.e. [Si][C_3]Cl, correspond to the propyl moieties present in the sample. The carbon and nitrogen contents found in the SIL were 9.028 % and 2.962 %, respectively, which reveals an increase in line with IL functionalized silica-gel samples.

Specific surface areas for functionalized and non-functionalized

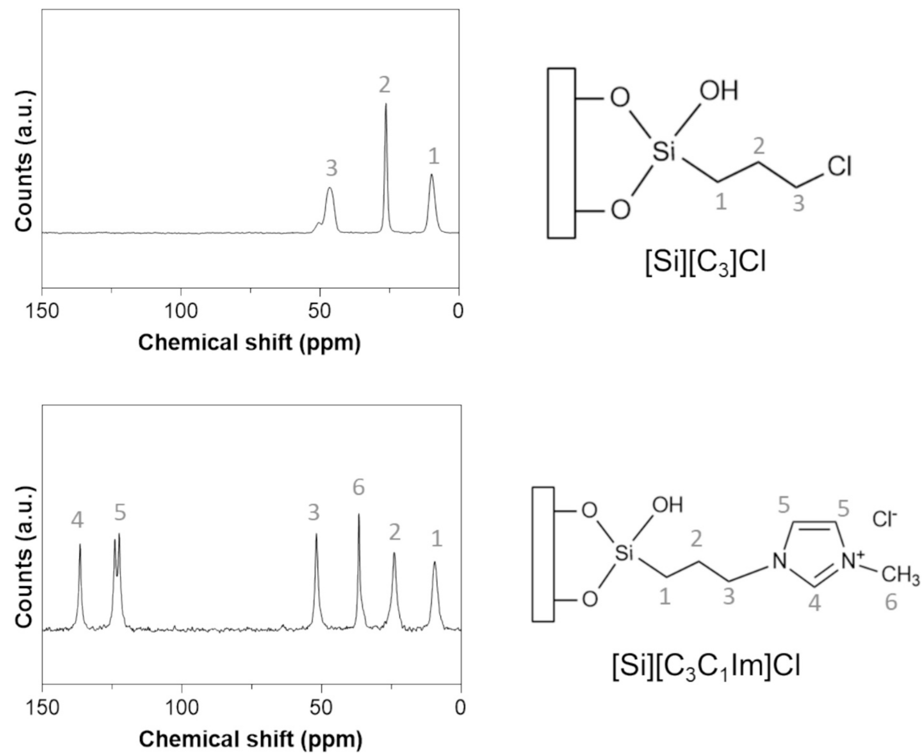

Fig. 1. Solid-state ^{13}C NMR spectra of $[Si][C_3]Cl$ and $[Si][C_3C_1Im]Cl$.

Table 2
Elemental analysis results, and BET surface area (S_{BET}), porosity volume (V_p) and pore diameter (D_p) values of activated silica, $[Si][C_3]Cl$ and $[Si][C_3C_1Im]Cl$.

Particles	%C	%H	%N	S_{BET} (m^2/g)	V_p (cm^3/g)	D_p (nm)
Activated Silica	–	–	–	466	0.729	5.1
$[Si][C_3]Cl$	6.452	1.558	–	345	0.369	3.8
$[Si][C_3C_1Im]Cl$	9.028	2.373	2.962	199	0.332	3.8

silica samples were measured via nitrogen adsorption using the BET (Brunauer-Emmett-Teller) method, as detailed in Table 2. The $[Si][C_3]Cl$ sample exhibited a lower specific surface area than the neat activated silica-gel but a higher value compared to the SIL. Silica has the highest value of pore diameter (5.1 nm), whereas both intermediate material and the SIL show a pore diameter of 3.8 nm. This indicates that the ILs fill the silica pores, causing a reduction in their volume and diameter.

Zeta potential measurements were carried out to assess the surface charge of both functionalized and non-functionalized silica-based materials. Fig. S2 (in the Supporting Information) contains the variation of zeta potential with pH for the activated silica, $[Si][C_3]Cl$ and $[Si][C_3C_1Im]Cl$. As predicted, the synthesized SIL displays higher PZC values (9.2) than both $[Si][C_3]Cl$ (4.3) and activated silica (3.9), consistent with the type of surface functionalization applied to the silica-gel samples [14,15]. This trend validates the presence of the imidazolium cation in the SIL and, therefore, the successful functionalization of the silica.

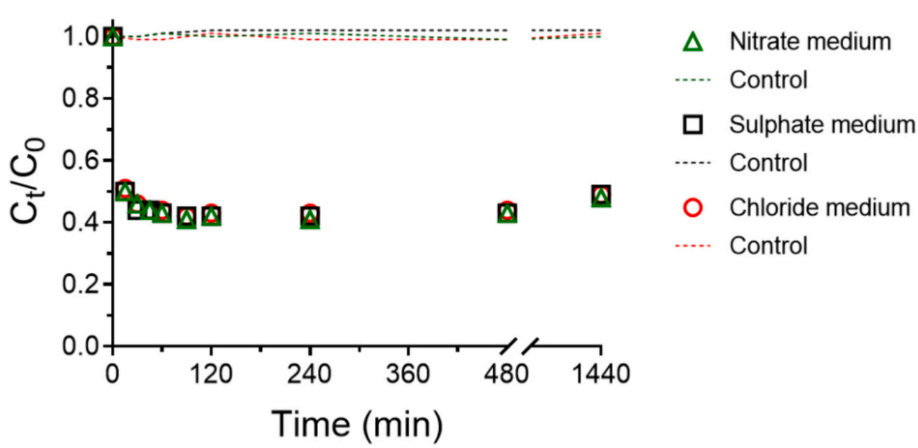

Fig. 2. Sorption kinetics of the SIL from single-element cobalt solutions consisting of different anionic media: Δ nitrate medium (–– control), □ sulphate medium (–– control) and ○ chloride medium (–– control) (1000 mL, 1 mg/L Co^{2+}, 0.001 M trisodium citrate, ultra-pure water, pH 6, 500 mg of SIL, 0–1440 min of contact time).

3.2. Influence of solution medium and time on sorption

The performance of the SIL synthesized in this work was firstly evaluated for cationic cobalt, in three different media depending on the anionic counterion employed: chloride, sulphate and nitrate. Fig. 2 displays the sorption kinetics of Co^{2+} complex in chloride, sulphate and nitrate media.

In terms of application, the sorption of Co^{2+} citrate complexes from chloride medium allows an equally efficient removal as from the two other media. Additionally, the chloride anion does not undergo speciation at the different solution pH values (contrary to the sulphate anion), which facilitates the interpretation of results. Lastly, as the counterion of the ionic liquid is chloride, in a chloride medium no ion exchange will occur with the anion from the medium and, therefore, the material can be regenerated later. Based on the obtained results, only chloride solutions were considered further on. Furthermore, the sorption kinetics is highly fast, reaching the maximum removal after 90 min. Therefore, a sorption time of 2 h was used in the following assays. These findings reinforce the potential of SILs for fast, selective recovery in chloride-rich effluents, aligning with the study's objective of developing a practical separation strategy for Co^{2+} and Ni^{2+}.

3.3. Influence of the citrate concentration on sorption

The effect of the citrate concentration on the removal percentage of Li^{+}, Co^{2+} and Ni^{2+} was studied using a multi-element solution. The results obtained are presented in Fig. 3.

There is a sharp increase in the cobalt and nickel removal percentage with the use of citrate concentration of 0.001 mol/L, after which the removal percentage steadily decreases again. This can be explained by the fact that the formation of Co^{2+} and Ni^{2+} citrate complexes requires a certain amount of citrate anions; a metal/ligand molar ratio of 1:1 and 1:2 is reported in the literature for the formation of Co^{2+} citrate complexes, such as $[Co(Cit)]^{-}$ and $[Co(Cit)_2]^{4-}$ [37,38], and Ni^{2+} citrate complexes, such as $[Ni(Cit)]^{-}$ and $[Ni(Cit)_2]^{4-}$ [39]. Thus, in the presence of citrate, it coordinates to cobalt and nickel, leading to the formation of ion pairs between the citrate complex and the SIL and, consequently, to an increase of the removal percentage. However, for citrate concentrations above 0.001 mol/L, there is a decrease in the removal percentage, which may be due to the competitive sorption between the citrate complexes of Co^{2+} and Ni^{2+} and the excess of citrate anions (in the form of $HCit^{2-}$ ions) [40,41].

This indicates that there is an optimal ligand-to-metal ratio that favors complex formation without overwhelming the sorbent with excess free citrate. Too little citrate leads to incomplete complexation, while too much introduces species that compete with metal-citrate complexes for active sites. These results highlight the critical balance between complex formation and competitive binding by free citrate species. This mechanistic insight also clarifies why no significant Li^{+} removal was observed, which is due to its inability to form comparable anionic complexes.

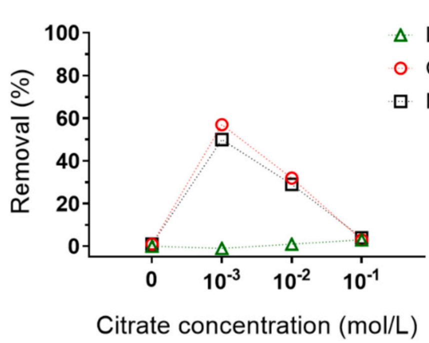

Fig. 3. Influence of the citrate concentration on the Δ lithium, ○ cobalt and □ nickel removal percentage by the SIL from multi-element solutions in chloride media (1000 mL, 1 mg/L of Li^{+}, Co^{2+} and Ni^{2+}, 0–0.1 mol/L trisodium citrate, ultra-pure water, pH 6, 500 mg of SIL, 120 min of contact time).

3.4. Regression model equations

Table S2 (in the Supporting Information) displays the results of removal (%) of Li^{+}, Co^{2+} and Ni^{2+}, after 2 h of exposure to the SIL, in the DoE conditions described in Table S1 (in the Supporting Information). The maximum removal achieved by SIL particles was observed for an initial metal concentration of 0.4 mg/L, pH 8 and SIL dosage of 1.0 g/L, with removal percentages of 86 % for Co^{2+} and 93 % for Ni^{2+}. The sorption of Li^{+} did not occur significantly in any of the experiments.

Some variability in the removal efficiency was observed across the different experiments, depending on the parameters tested (pH, sorbent dose, and initial metal concentration). Therefore, applying RSM to optimize these experimental parameters is essential. Since no sorption of Li^{+} occurred, only experimental results associated with Co^{2+} and Ni^{2+} were analysed and fitted to the mathematical model.

The linear, quadratic, and combined effects of the variables on the removal efficiency of Co^{2+} and Ni^{2+} are shown in Fig. 4, with results obtained at a 95 % confidence level. In the Pareto chart, the letters A, B, and C correspond to the variables pH, sorbent dose, and initial concentrations of Co^{2+} and Ni^{2+}. Variables located before the red line are significant for the response (p-value <0.05). The green bars indicate a positive effect (the response increases with the variable), grey bars represent non-significant variables, and red bars show a negative effect (the response decreases as the variable increases). The p-values for the fitted models are presented in the ANOVA tables (Tables S3 and S4 in the Supplementary Material).

The data show that the effect of variables in the removal (%) changes slightly according to the chemical element under analysis. The most significant factors for both Co^{2+} and Ni^{2+} removal are the "dose of sorbent" (with positive contribution), the quadratic effects of "pH" (with negative contribution) and the interaction between the "pH" and the "initial concentration" (also with negative contribution). Additionally, for Co^{2+}, the "pH" has a positive effect on the response, while for Ni^{2+} the effect of "initial concentration" is more significant, with a negative effect on the response. Thus, the increase in removal percentage depends on a combination of high pH, high dose of sorbent and low initial concentration of the elements. As the solution pH increases, the Co^{2+} and Ni^{2+} citrate complexes tend to be more negatively charged [37], increasing the interaction with the positively charged SIL. Regarding the dose of sorbent, the number of binding sites available for sorption increases with the increase in mass; at lower metals concentration in solution, the active sites take longer to become saturated.

The reduced models presented in Table 3 were generated using only the significant variables. These models are represented by the real values of the independent variables. The fit quality between the experimental and predicted values is determined by the coefficient of determination (R^2) and the adjusted coefficient of determination (R^2_{adj}).

With high R^2 (0.9303) and R^2_{adj} (0.8915) values, the reduced model for Ni^{2+} demonstrates a good fit and model robustness, ensuring accurate response predictions. The value of R^2 for Co^{2+} function was also good, but lower than that for Ni^{2+}. Despite that, the values of R^2 and R^2_{adj} validate the good robustness of the model.

3.5. Application of response surface methodology for optimizing experimental parameters

Fig. 5 shows the 3D response surface plots for Co^{2+} and Ni^{2+} removal by the SIL, respectively. The interactive effects of the different variables confirm that higher removal percentages are obtained at higher pH values, lower metals concentrations, and with the maximum sorbent dose. The models not only capture the individual effects of the variables but also reveal important synergies between them.

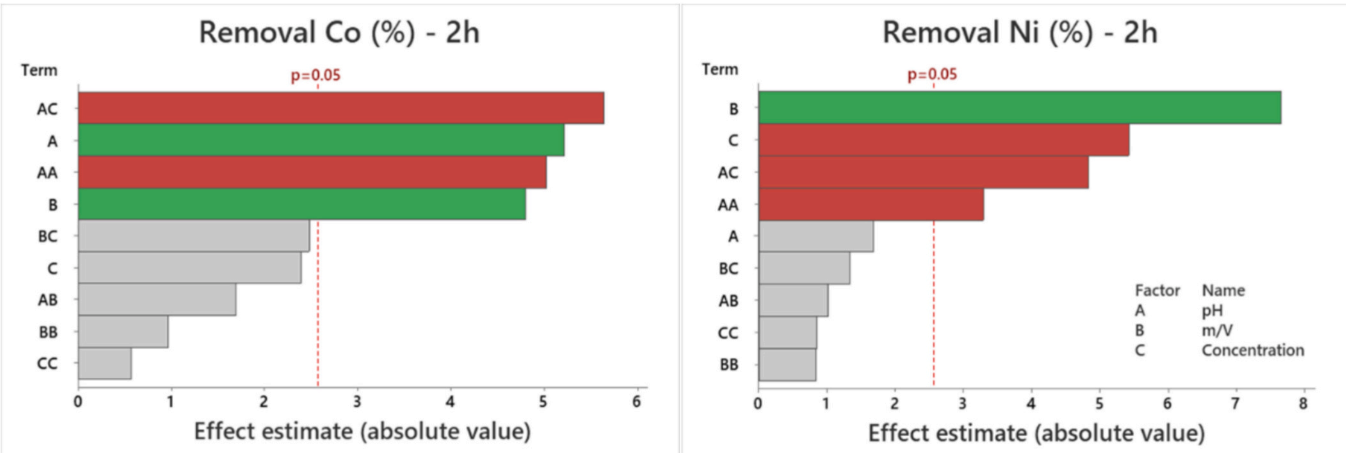

Fig. 4. Pareto chart showing the impact of variables on the removal percentage of Co^{2+} and Ni^{2+} after 2 h of exposure. A corresponds to the solution pH, B to the sorbent dose (g/L), and C to the initial concentration of metals (mg/L). Variables with values below the dashed line are considered non-significant.

Table 3
Reduced models of the removal % at 2 h, with the corresponding R^2 and adjusted R^2 values, as determined by the significant variables (p-value <0.05).

Co^{2+}	Response reduced model	Removal (%) = − 174.53 + 59.89 pH + 18.98 Mass + 53.20 Concentration - 9.85 pH*Concentration - 3.58 pH*pH
	R^2	0.8806
	R^2_{adj}	0.8143
Ni^{2+}	Response reduced model	Removal (%) = − 60.54 + 32.25 pH + 24.03 Mass + 29.64 Concentration - 6.71 pH*Concentration - 1.91 pH*pH
	R^2	0.9303
	R^2_{adj}	0.8915

The optimization of the operation parameters allows to maximize the removal of the metals under study. Even though the removal efficiency from the Box-Behnken design experiments suggests no affinity of Li^+ for SIL particles, this element was found in all the experimental solutions. The optimal experimental conditions determined by RSM are presented in Table 4. The optimal values for the variables were a pH of 7.8, sorbent dose of 1.5 g/L, and an initial concentration of 0.4 mg/L, with expected removal of 94 % for Co^{2+} and 100 % for Ni^{2+}.

These conditions are consistent with the behavior of citrate-metal complexes and the positively charged nature of the SIL surface at near-neutral pH. At pH 7.8, the cobalt and nickel citrate complexes are predominantly in their anionic forms, which enhances electrostatic interactions with the imidazolium cations on the SIL. Additionally, a higher sorbent dose increases the number of available active sites, contributing to the high removal rates. The lower initial concentration likely favors sorption due to reduced competition for active sites and more favorable concentration gradients. Together, these factors create ideal conditions for efficient and selective sorption, which is advantageous for practical applications in treating dilute industrial effluents.

3.6. *Validation of the conditions determined by DoE and impact of the matrix on Co^{2+} and Ni^{2+} removal*

An assay under the optimum conditions was performed to confirm the predictions of removal percentages determined by DoE. The results presented in Table 4 show that the removal percentages obtained experimentally using the SIL were closer to those obtained by DoE, but slightly inferior for Ni^{2+}. This slight deviation may be attributed to experimental variability or to minor competitive effects not fully captured by the model.

Removal efficiencies were also assessed in bottled water and synthetic solutions with salinities of 15 (typical for coastal and transitional systems) and 30 (representative of seawater). The removal percentages in these different matrices are shown in Table 4. The removal efficiencies in ultra-pure and bottled water were similar; however, in saline water no sorption occurred, indicating that there was competition for the binding sites with other anions present in this matrix, as well as increased ionic strength reducing electrostatic interactions. The findings of this study suggest that the use of SIL particles for removing Co^{2+} and Ni^{2+} is mainly applicable to less complex matrices in aquatic systems or industrial effluents.

The observed similarity between Co^{2+} and Ni^{2+}, both in removal percentages and in how the studied variables influence their removal, suggests that the sorption mechanism of the elements, in the form of anionic citrate complexes, is indeed similar. This mechanism is primarily governed by electrostatic interactions between the negatively charged Co^{2+} and Ni^{2+} citrate complexes and the positively charged imidazolium-based SIL surface. At pH values below the material's point of zero charge (PZC = 9.2), the SIL surface remains positively charged, enhancing sorption via Coulombic attraction. This aligns with the optimal pH identified in this study (around 7.8), where the citrate-metal complexes are predominantly in their anionic forms. The comparable behavior of Co^{2+} and Ni^{2+} can be attributed to their similar ionic radii, oxidation states, and coordination chemistry. Overall, the uptake of these metals appears to be driven by complexation-assisted electrostatic sorption under near-neutral pH, where both the SIL charge and complex speciation favor interaction. While these observations strongly support an electrostatic interaction mechanism, we acknowledge that further studies involving advanced spectroscopic or modeling techniques are needed to conclusively confirm the sorption mechanism.

Although not evaluated in the present study, SILs are known to be regenerable using mild acidic treatments. For instance, Van Roosendael et al. [40] demonstrated that metal-loaded SILs can be effectively regenerated using HNO_3 or NH_4Cl without compromising their structural integrity or sorption capacity. Given the similar chemical structure of the SIL used in this work, particularly its chloride-based composition, analogous regeneration strategies are expected to be effective. In particular, stripping with NH_4Cl solution would avoid anion exchange and help preserve the chloride counterion of the SIL, supporting its reusability in multiple sorption cycles. We emphasize that this regeneration strategy is proposed based on literature findings and was not experimentally verified in this study. This highlights the potential of the developed SIL not only for efficient Co^{2+} and Ni^{2+} separation but also for integration into circular and sustainable recovery processes.

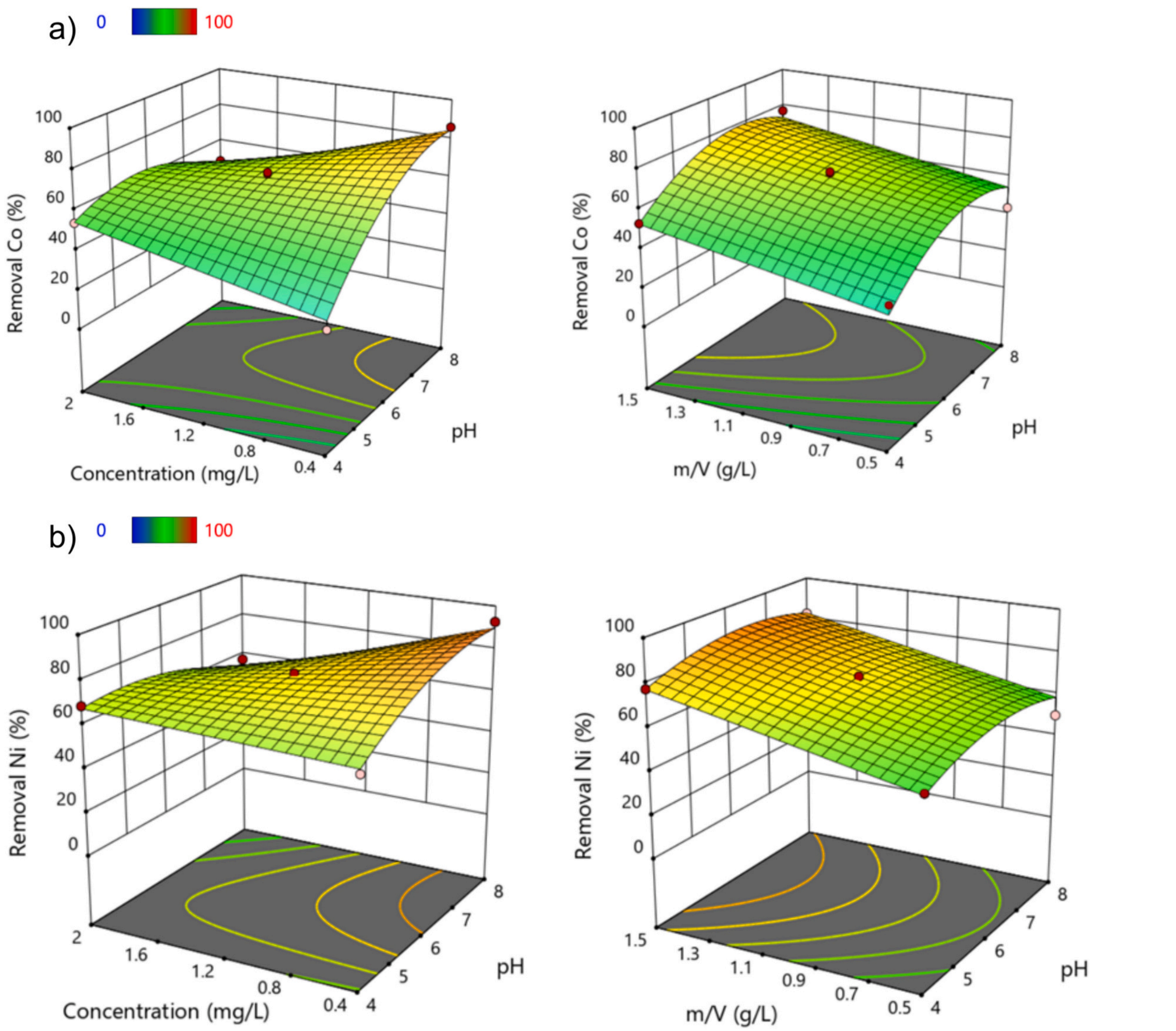

Fig. 5. 3-D Response Surfaces derived from the reduced models after 2 h of Co^{2+} exposure (a) and Ni^{2+} exposure (b) to [Si][C_3C_1Im]Cl, in function of the concentration and pH (on left) and the sorbent dose and pH (on right).

Table 4
Comparison of the removal (%) of Co^{2+} and Ni^{2+} obtained through DoE and experimentally.

Chemical element	Optimum conditions			% Removal DoE	% Removal Experimental			
	pH	Dose of sorbent (g/L)	Initial concentration (mg/L)		Ultra-pure water	Mineral water	Salinity 15	Salinity 30
Co^{2+}	7.8	1.5	0.4	94	95	89	0	0
Ni^{2+}				100	95	92	1	0

3.7. Ecotoxicological impacts on mussels

Biochemical analyses were performed to assess metabolic efficiency and oxidative stress in *Mytilus galloprovincialis* following exposure to the sorbent [Si][C3C1Im]Cl, providing specific insight into its ecotoxicological impact. The results obtained demonstrated no significant differences among tested concentrations, indicating no impacts resulting from the exposure to this sorbent (Figs. 6 and 7).

ETS activity reflects the metabolic capacity of organisms and involves mitochondrial protein complexes responsible for energy production [42]. Under pollutant-induced stress, bivalves may initially reduce their metabolism to limit contaminant uptake [43], but if the stress exceeds a threshold, metabolic activity may increase to support defense mechanisms [44]. However, in the present study, neither a significant suppression nor stimulation of ETS activity was observed in mussels exposed to varying concentrations of SIL. This suggests that the tested concentrations did not elicit a strong enough physiological stress response to alter the metabolic capacity of the organisms within the timeframe of acute exposure. These findings imply a limited impact of SIL, under the tested conditions, on the mitochondrial energy production pathway in mussels.

The absence of significant changes in metabolic activity was further supported by the stable levels of total PROT content across treatments. This suggests that mussels maintained a balance between protein synthesis and degradation, implying that proteins were neither being excessively catabolized for energy nor synthesized in large amounts for

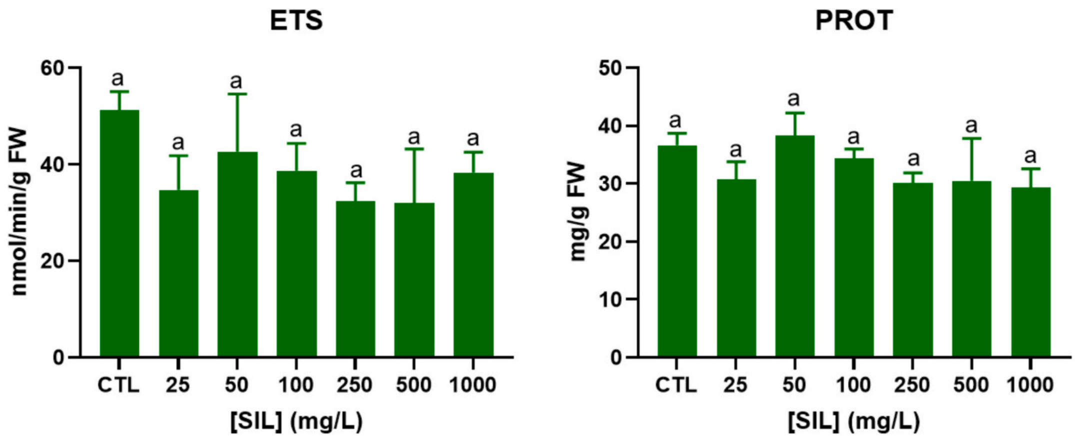

Fig. 6. Electron transport system (ETS) activity (on left) and total protein (PROT) content (on right) in *M. galloprovincialis* after 7 days of exposure to SIL.

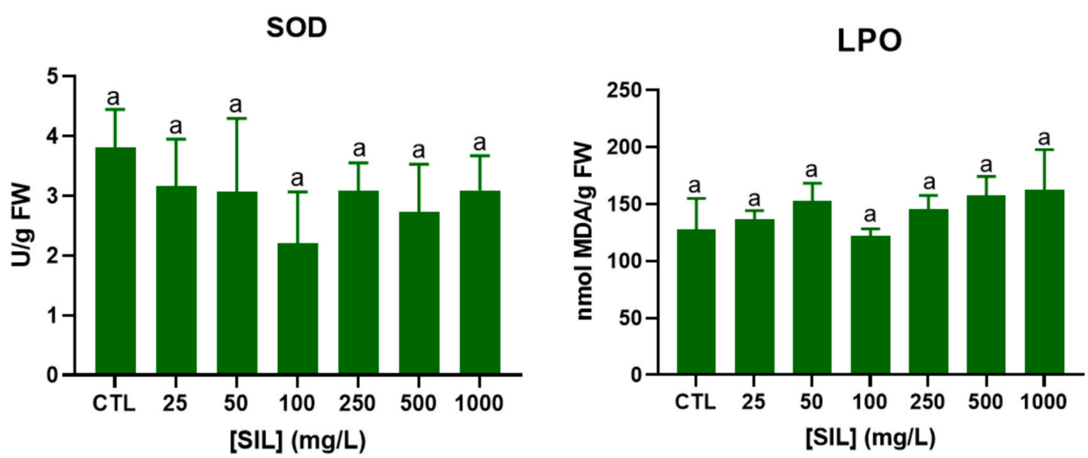

Fig. 7. Superoxide dismutase (SOD) activity (on left) and lipid peroxidation (LPO) levels (on right) in *M. galloprovincialis* after 7 days of exposure to SIL.

stress-related responses. The unaltered PROT levels also indicate that the organisms were not experiencing substantial physiological stress, as no increased demand for protein-based enzymatic defense mechanisms was evident. Together with the unchanged ETS activity, these results suggest that the tested concentrations of SIL did not trigger a metabolic or proteomic response in mussels during the acute exposure period, reinforcing the interpretation that the exposure did not compromise their cellular homeostasis.

Pollutant exposure often leads to excessive production of reactive oxygen species (ROS), primarily from the mitochondrial ETS, which can cause oxidative damage to proteins, lipids, and DNA if not neutralized by antioxidant defenses [41]. In the present study, however, no significant lipid peroxidation (LPO) was detected at any of the tested SIL concentrations, suggesting the absence of oxidative damage to cellular membranes. This aligns with the unaltered ETS activity, indicating no excessive mitochondrial ROS production. Furthermore, superoxide dismutase (SOD) activity remained stable across the increasing SIL concentration gradient. As a primary antioxidant enzyme responsible for the dismutation of superoxide anions into oxygen and hydrogen peroxide, SOD plays a crucial role in mitigating oxidative stress by neutralizing one of the most reactive ROS species [41]. The unchanged SOD activity observed in this study reinforces the conclusion that SIL exposure did not stimulate ROS overproduction or trigger the activation of antioxidant defense pathways.

Thus, the presence of SIL at concentrations up to 1 g/L does not exhibit toxicity levels capable of disrupting the physiological homeostasis of *M. galloprovincialis*. The lack of significant changes in ETS activity, total PROT content, antioxidant enzyme response, and LPO collectively indicates that SIL did not impair mitochondrial function, trigger oxidative stress, or cause cellular damage in *M. galloprovincialis* under acute exposure conditions. These results suggest a limited ecotoxicological risk of SIL to mussels at the tested concentrations, at least in the short term. Similar outcomes have been reported in previous studies involving imidazolium-based ionic liquids, further supporting the low acute toxicity of these compounds under the tested conditions [23].

4. Conclusions

This work demonstrated the efficiency of an imidazolium-based SIL for removing citrate-coordinated Co^{2+} and Ni^{2+} from aqueous solutions. In the absence of citrate, no metal removal was observed, highlighting the importance of complexing the metals into anionic forms to enable sorption. The process exhibited rapid kinetics, with equilibrium achieved in less than 2 h, which can contribute to reduced energy consumption and operational costs in industrial applications.

Optimization using a Box-Behnken DoE approach identified pH and SIL dose as key variables. Under optimal conditions (pH 7.8, 1.5 g/L SIL, 0.4 mg/L metals), removal efficiencies reached 94 % for Co^{2+} and 100 % for Ni^{2+}. While excellent efficiencies were observed in ultra-pure and bottled waters (between 89 % and 95 %), the efficiency decreased significantly in saline matrices, indicating limitations in more complex aqueous systems.

Ecotoxicological assays using *Mytilus galloprovincialis* showed no significant biochemical changes at SIL concentrations up to 1 g/L, supporting the material's environmental safety.

Overall, the SIL developed in this study offers a fast, effective, and environmentally safe approach for Co^{2+} and Ni^{2+} recovery from low-salinity water matrices, including industrial effluents, and contributes to the development of more sustainable processes for critical metal recovery from secondary sources.

Supporting information

Detailed synthesis procedure, quantification techniques, RSM equations, description of the experimental conditions according to the Box-Behnken design and removal % achieved, FTIR spectra, graphs of zeta potential as a function of pH, influence of solution medium and time on sorption, graphs of biomarkers quantification.

CRediT authorship contribution statement

Joana C. Almeida: Writing – original draft, Methodology, Formal analysis, Data curation. **Celso E.D. Cardoso:** Writing – original draft, Investigation, Formal analysis, Data curation. **Rosa Freitas:** Writing – review & editing, Supervision, Funding acquisition, Conceptualization. **Tito Trindade:** Writing – review & editing, Resources, Funding acquisition. **Mara G. Freire:** Resources, Investigation, Funding acquisition, Conceptualization. **Eduarda Pereira:** Writing – review & editing, Supervision, Resources, Investigation, Funding acquisition, Conceptualization.

Declaration of competing interest

The authors declare that they have no known competing financial interests or personal relationships that could have appeared to influence the work reported in this paper.

Acknowledgment

This work is funded by national funds through FCT – Fundação para a Ciência e a Tecnologia I.P., under the project/grant UID/50006 + LA/P/0094/2020, UIDB/50006/2020, UIDP/50006/2020, and LA/P/0008/2020. This work was also developed within the scope of the project CICECO - Aveiro Institute of Materials, UIDB/50011/2020 (DOI 10.54499/UIDB/50011/2020), UIDP/50011/2020 (DOI 10.54499/UIDP/50011/2020) and LA/P/0006/2020 (DOI 10.54499/LA/P/0006/2020), financed by national funds through the FCT/MCTES (PIDDAC). This work was also funded by national funds through FCT – Fundação para a Ciência e a Tecnologia I.P., under the project/grant UID/50006 + LA/P/0094/2020 (doi.org/10.54499/LA/P/0094/2020). The NMR spectrometers are part of the National NMR Network (PTNMR) and are partially supported by Infrastructure Project N° 022161 (co-financed by FEDER through COMPETE 2020, POCI and PORL and FCT through PIDDAC). Joana C. Almeida thanks FCT/MCTES and ESF (European Social Fund) through NORTE 2020 (Programa Operacional Região Norte) for the PhD grant SFRH/BD/139471/2018. Celso E. D. Cardoso thank FCT/MCTES (Fundação para a Ciência e Tecnologia and Ministério da Ciência, Tecnologia e Ensino Superior) and ESF (European Social Fund) through NORTE 2020 (Programa Operacional Região Norte) for the PhD grant 2021.06684.BD.

Appendix A. Supplementary data

Supplementary data to this article can be found online at https://doi.org/10.1016/j.susmat.2025.e01619.

Data availability

Data will be made available on request.

References

[1] B. Scrosati, J. Garche, Lithium batteries: status, prospects and future, J. Power Sources 195 (2010) 2419–2430.
[2] European Commission, Report on Critical Raw Materials and the Circular Economy, 2018.
[3] R. Krishnan, G. Gopan, A comprehensive review of lithium extraction: from historical perspectives to emerging technologies, storage, and environmental considerations, Clean. Eng. Technol. 20 (2024) 100749.
[4] B. Swain, Recovery and recycling of lithium: a review, Sep. Purif. Technol. 172 (2017) 388–403.
[5] H. Wang, K. Huang, Y. Zhang, X. Chen, W. Jin, S. Zheng, Y. Zhang, P. Li, Recovery of Lithium, nickel, and cobalt from spent Lithium-ion battery powders by selective Ammonia leaching and an adsorption separation system, ACS Sustain. Chem. Eng. 5 (2017) 11489–11495.
[6] W. Mrozik, M.A. Rajaeifar, O. Heidrich, P. Christensen, Environmental impacts, pollution sources and pathways of spent lithium-ion batteries, Energy Environ. Sci. 14 (2021) 6099–6121.
[7] K. Momina, Ahmad, feasibility of the adsorption as a process for its large scale adoption across industries for the treatment of wastewater: research gaps and economic assessment, J. Clean. Prod. 388 (2023) 136014.
[8] D.-I. Ferţu, A.-A. Ciobanu, I.G. Cara, I. Motrescu, I. Ahmad, G. Nacu, L. Bulgariu, Circular approach of using soybean biomass for the removal of toxic metal ions from wastewater, Water 16 (2024) 3663.
[9] A.-A. Ciobanu, A.-R. Lucaci, L. Bulgariu, Efficient metal ions biosorption on red and green algae biomass: isotherm, kinetic and thermodynamic study, J. Appl. Phycol. 36 (2024) 3809–3827.
[10] N. Rahman, M. Nasir, N -(((2-((2-Aminoethyl)amino)ethyl)amino)methyl)-4-sulfamoylbenzamide impregnated hydrous zirconium oxide as a novel adsorbent for removal of Ni(II) from aqueous solutions: optimization of variables using central composite design, ACS Omega 4 (2019) 2823–2832.
[11] M.H. Salmani, M.H. Ehrampoush, H. Eslami, B. Eftekhar, Synthesis, characterization and application of mesoporous silica in removal of cobalt ions from contaminated water, Groundw. Sustain. Dev. 11 (2020) 100425. https://linkinghub.elsevier.com/retrieve/pii/S2352801X19301316.
[12] M.A.A. Ebrahim, T. Ebadi, Experimental design study of nickel removal from aqueous solution by activated carbon and its pore size distribution modification using carbon dioxide gasification for enhancing adsorption efficiency, Desalin. Water Treat. 205 (2020) 175–188.
[13] H. Ahmad, R.A. Khan, B.H. Koo, A. Alsalme, Separation of heavy metals by amino acid functionalized polymer: experimental and theoretical insights, J. Phys. Chem. Solids 171 (2022) 111026.
[14] H.F.D. Almeida, M.C. Neves, T. Trindade, I.M. Marrucho, M.G. Freire, Supported ionic liquids as efficient materials to remove non-steroidal anti-inflammatory drugs from aqueous media, Chem. Eng. J. 381 (2020) 122616–122626.
[15] S.C. Bernardo, B.R. Araújo, A.C.A. Sousa, R.A. Barros, A.C. Cristovão, M.C. Neves, M.G. Freire, Supported ionic liquids for the efficient removal of acetylsalicylic acid from aqueous solutions, Eur. J. Inorg. Chem. 2020 (2020) 2380–2389.
[16] O. Lanaridi, A.R. Sahoo, A. Limbeck, S. Naghdi, D. Eder, E. Eitenberger, Z. Csendes, M. Schnürch, K. Bica-Schröder, Toward the recovery of platinum group metals from a spent automotive catalyst with supported ionic liquid phases, ACS Sustain. Chem. Eng. 9 (2021) 375–386.
[17] Z. Lei, B. Chen, Y.M. Koo, D.R. Macfarlane, Introduction: Ionic Liquids, Chem. Rev. 117 (2017) 6633–6635.
[18] S.P.M. Ventura, F.A. e Silva, M.V. Quental, D. Mondal, M.G. Freire, J.A. P. Coutinho, Ionic-liquid-mediated extraction and separation processes for bioactive compounds: past, present, and future trends, Chem. Rev. 117 (2017) 6984–7052.
[19] A.Q. Pedro, J.A.P. Coutinho, M.G. Freire, Immobilization of ionic liquids, types of materials, and applications, in: Encycl. Ion. Liq, Springer, Singapore, 2019, pp. 1–12.
[20] P.A. Yudaev, E.M. Chistyakov, Ionic liquids as components of systems for metal extraction, ChemEngineering 6 (2022) 1–22.
[21] A.V. Panteleimonov, M.O. Onizhuk, I.V. Khristenko, I.I. Chuiko, O.S. Tkachenko, Y. Gushikem, Y.V. Kholin, Adsorption of transition metal chlorides by silica with grafted 1-n-Propyl-3-Methylimidazolium chloride, J. Braz. Chem. Soc. 26 (2015) 1160–1170.
[22] R. Hanzel, P. Rajec, Sorption of cobalt on modified silica gel materials, J. Radioanal. Nucl. Chem. 246 (2000) 607–615.
[23] M. Vieira Sanches, M. Oliva, A. Mezzetta, L. Guazzelli, L. De Marchi, R. Freitas, C. Pretti, In vitro screening of imidazolium and pyrrolidinium based ionic liquids toxicity on subcellular fractions of the Mediterranean mussel Mytilus galloprovincialis, Environ. Toxicol. Pharmacol. 104 (2023) 104305.
[24] M.V. Sanches, R. Freitas, M. Oliva, A. Cuccaro, G. Monni, A. Mezzetta, L. Guazzelli, C. Pretti, Toxicity of ionic liquids in marine and freshwater microorganisms and invertebrates: state of the art, Environ. Sci. Pollut. Res. 30 (2023) 39288–39318.
[25] V. Thamke, P. Singh, S. Pal, M. Chaudhary, K. Kumari, I. Bahadur, R.S. Varma, Current toxicological insights of ionic liquids on various environmental living forms, J. Environ. Chem. Eng. 10 (2022) 107303, https://doi.org/10.1016/j.jece.2022.107303.
[26] S.P.M. Ventura, A.M.M. Gonçalves, F. Gonçalves, J.A.P. Coutinho, Assessing the toxicity on [C3mim][Tf2N] to aquatic organisms of different trophic levels, Aquat. Toxicol. 96 (2010) 290–297, https://doi.org/10.1016/j.aquatox.2009.11.008.
[27] J.S. Strehse, E. Maser, Marine bivalves as bioindicators for environmental pollutants with focus on dumped munitions in the sea: a review, Mar. Environ. Res. 158 (2020) 105006–105015.

[28] A. Witek-Krowiak, K. Chojnacka, D. Podstawczyk, A. Dawiec, K. Pokomeda, Application of response surface methodology and artificial neural network methods in modelling and optimization of biosorption process, Bioresour. Technol. 160 (2014) 150–160.

[29] S.L.C. Ferreira, R.E. Bruns, H.S. Ferreira, G.D. Matos, J.M. David, G.C. Brandão, E. G.P. da Silva, L.A. Portugal, P.S. dos Reis, A.S. Souza, W.N.L. dos Santos, Box-Behnken design: an alternative for the optimization of analytical methods, Anal. Chim. Acta 597 (2007) 179–186.

[30] E. Fabre, B. Henriques, T. Viana, J. Pinto, M. Costa, N. Ferreira, D. Tavares, C. Vale, J. Pinheiro-Torres, E. Pereira, Optimization of Nd(III) removal from water by Ulva sp. and Gracilaria sp. through response surface methodology, J. Environ. Chem. Eng. 9 (2021) 105946–105954.

[31] C.E.D. Cardoso, J.C. Almeida, J. Rocha, E. Pereira, Application of box-Behnken design to optimize the phosphorus removal from industrial wastewaters using magnetic nanoparticles, Environ. Sci. Pollut. Res. 32 (2025) 6804–6816, https://doi.org/10.1007/s11356-025-36152-6.

[32] M. Nasir, M. Bharti, N. Rahman, M.S. Samdani, M. Alam, Environmentally Sustainable Hydrous Zirconium Oxide–Inulin as an Efficient Adsorbent for Ciprofloxacin Removal: Mechanistic and Thermodynamic Insights via Statistical Physics and Fractal-like Kinetic Modeling, Langmuir 41 (2025) 12199–12217.

[33] H. Qiu, S. Jiang, X. Liu, N-Methylimidazolium anion-exchange stationary phase for high-performance liquid chromatography, J. Chromatogr. A 1103 (2006) 265–270.

[34] A. Kalinowska, M. Szopińska, S. Chmiel, M. Kończak, Ż. Polkowska, W. Artichowicz, K. Jankowska, A. Nowak, A. Łuczkiewicz, Heavy metals in a high Arctic fiord and their introduction with the wastewater: a case study of Adventfjorden-Longyearbyen system, Svalbard, Water 12 (2020) 794, https://doi.org/10.3390/w12030794.

[35] S. Ishaq, G. Jabeen, M. Arshad, Z. Kanwal, F. Un Nisa, R. Zahra, Z. Shafiq, H. Ali, K. B. Samreen, F. Manzoor, Heavy metal toxicity arising from the industrial effluents repercussions on oxidative stress, liver enzymes and antioxidant activity in brain homogenates of Oreochromis niloticus, Sci. Rep. 13 (2023) 19936, https://doi.org/10.1038/s41598-023-47366-4.

[36] M. Andrade, A.M.V.M. Soares, M. Solé, E. Pereira, R. Freitas, Salinity influences on the response of Mytilus galloprovincialis to the rare-earth element lanthanum, Sci. Total Environ. 794 (2021) 148512–148521.

[37] A.C. Frank, P.T.A. Sumodjo, Electrodeposition of cobalt from citrate containing baths, Electrochim. Acta 132 (2014) 75–82.

[38] A.V. Chzhan, S.A. Podorozhnyak, G.S. Patrin, R.Y. Rudenko, V.V. Onufrienok, Influence of solution acidity on growth kinetics, structure and magnetic properties of Co-P films, obtained by chemical deposition, J. Phys. Conf. Ser. 1389 (2019) 012116–012122.

[39] G.R. Hedwig, J.R. Liddle, R.D. Reeves, Complex formation of nickel(II) ions with citric acid in aqueous solution: a potentiometric and spectroscopic study, Aust. J. Chem. 33 (1980) 1685–1693.

[40] S. Van Roosendael, J. Roosen, D. Banerjee, K. Binnemans, Selective recovery of germanium from iron-rich solutions using a supported ionic liquid phase (SILP), Sep. Purif. Technol. 221 (2019) 83–92.

[41] C. Gervais, C.A. Grissom, N. Little, M.J. Wachowiak, Cleaning marble with ammonium citrate, Stud. Conserv. 55 (2010) 164–176.

[42] I.M. Sokolova, Ectotherm mitochondrial economy and responses to global warming, Acta Physiol. 237 (2023) 1–13.

[43] Â. Almeida, R. Freitas, V. Calisto, V.I. Esteves, R.J. Schneider, A.M.V.M. Soares, E. Figueira, Chronic toxicity of the antiepileptic carbamazepine on the clam Ruditapes philippinarum, Comp. Biochem. Physiol. Part C Toxicol. Pharmacol. 172–173 (2015) 26–35.

[44] M. Andrade, A.M.V.M. Soares, M. Solé, E. Pereira, R. Freitas, Threats of pollutants derived from electronic waste to marine bivalves: the case of the rare-earth element yttrium, Environ. Toxicol. Chem. 42 (2023) 166–177.